ARCHIVES OF ELECTRICAL ENGINEERING VOL. 61(2), pp. 165-188 (2012)

DOI 10.2478/v10171-012-0015-1

Observer-based fault diagnosis and field oriented fault tolerant control of induction motor with stator inter-turn fault

DJILALI TOUMI[1], MOHAMED SEGUIER BOUCHERIT[2], MOHAMED TADJINE[2]

[1]*Electrical Engineering Department*
Ibn Khaldoun University, BP 78 Tiaret Algeria

[2]*Process Control Laboratory, 10 Avenue H. Badi BP 182*
Automatic control department, ENP Alger, Algeria
e-mail: {toumi_dj/ms_boucherit/tadjine@yahoo.fr

(Received: 21.09.2011, revised: 19.12.2011)

Abstract: This paper describes a *fault-tolerant controller* (FTC) of *induction motor* (IM) with inter-turn short circuit in stator phase winding. The *fault-tolerant* controller is based on the *indirect rotor field oriented control* (IRFOC) and an observer to estimate the motor states, the amount of turns involved in short circuit and the current in the short circuit. The proposed fault controller switches between the control of the two components of measured stator current in the synchronously rotating reference frame and the control of the two components of estimated current in the case of faulty condition when the estimated current in the short circuit is not destructive of motor winding. This technique is used to eliminate the speed and the rotor flux harmonics and to assure the decoupling between the rotor flux and torque controls. The results of the simulation for controlling the speed and rotor flux of the IM demonstrate the applicability of the proposed FTC.

Key words: induction motor, short circuit, vector control, fault-tolerant control, fault diagnostic

1. Introduction

Induction machine drives are the most widely used in the adjustable speed drives field. The advantages of this solution are, on one hand, their relatively low cost, simple construction and easy maintenance. On the other hand, progress made in control and algorithm implementation technologies enabled these drives to have high dynamic and static performances. They have reached a high degree of maturity and become standard industrial solutions for a wide range of power and applications (robotics, railway transportation, marine propulsion, wind power generation) [1-3].

The possibility for electrical machine faults is unavoidable. Many components of the induction machine are susceptible to failures, the stator windings are subject to insulation breakdown, the bars and end rings of the squirrel cage are subject to failures, machine bearings are subject to excessive wear and damage etc, all caused by a combination of thermal, electrical, mechanical, magnetic and environmental stresses [4-7].

Fault diagnosis of rotating electrical motors has received intense research interest [8-11], because of its great influence on the operational continuation of some industrial processes. Correct diagnosis and early detection of incipient faults result in fast unscheduled maintenance and short down time for the process under consideration. They also avoid harmful, sometimes devastative, consequences and help reducing financial loss. Condition monitoring systems include both measurement hardware and software that acquire and interpret signals generated by the machine being monitored [12, 13].

In recent years, *fault detection and isolation* (FDI) has been studied extensively [14-17]. Advances in control theory have greatly speed up the development of FDI of electrical machines and various approaches have been proposed. Among these approaches, observer based FDI is an effective one and has been widely studied especially in last years [3, 18-20]. The fundamental purpose of a FDI scheme is to generate an alarm when a fault occurs and also, if it is possible, to locate the fault or to estimate its magnitude [16, 18, 20]. Another versions usually consist in designing a supervisory unit which, on the basis of the information provided by the FDI system, achieves control reconfiguration to compensate for the effect of the fault and guarantee fulfillment of performance constraints.

Many effort in the control community have been recently devoted to study FTC system associated with the IFOC to preserve pre-specified performance and to compensate harmonics in the currents, torque, speed and flux, at the presence of rotor or stator faults [16, 21-24].

In this work, we propose a FTC of IM drive to reduce the effect of inter-turn short circuit in stator phase winding, aiming at decoupling between torque and rotor flux control and at eliminating harmonics from induction machine states. A bilinear observer is used to estimate the fraction of the short circuit turns, the short circuit current and the other $d-q$ axis components of stator current directly responsible for production of rotor flux and electromagnetic torque. When the IM operates in faulty condition, then the latter currents are controlled instead of measured currents in order to compensate the fault effects when the estimated short circuit current is not exceeding the acceptable level assuring the machine operation with degraded performance until its repair or his exchange.

2. Healthy induction motor model

2.1. Machine equations in abc variables

The induction motor model presented in this part considers that the stator and the rotor consists of the three sinusoidally distributed windings displaced by electrical angle of 120°, with the following general assumptions: The magnetic saturation is negligible, the air gap is uniform, the windings are sinusoidally distributed, the permeability of iron parts are supposed infinite,…

In this paper all matrices and vectors are written with bold letters, to distinguish these from scalar values.

The voltage equations for the stator and rotor winding for symmetrical induction motor can be written as:

$$\begin{aligned} \boldsymbol{v}_{sabc} &= \mathbf{r}_s\, \boldsymbol{i}_{sabc} + \frac{d\boldsymbol{\phi}_{sabc}}{d\,t}, \\ 0 &= \mathbf{r}_r\, \boldsymbol{i}_{rabc} + \frac{d\boldsymbol{\phi}_{rabc}}{d\,t}. \end{aligned} \tag{1}$$

The equations of the stator and rotor flux linkages can be expressed as follows:

$$\begin{aligned} \boldsymbol{\phi}_{sabc} &= \mathbf{l}_s\, \boldsymbol{i}_{sabc} + \mathbf{m}_{sr}(\theta)\, \boldsymbol{i}_{rabc}, \\ \boldsymbol{\phi}_{rabc} &= \mathbf{l}_r\, \boldsymbol{i}_{rabc} + \mathbf{m}_{sr}^{t}(\theta)\, \boldsymbol{i}_{sabc}. \end{aligned} \tag{2}$$

Where $\boldsymbol{v}_{sabc} = [v_{sa} \quad v_{sb} \quad v_{sc}]^t$, $\boldsymbol{i}_{sabc} = [i_{sa} \quad i_{sb} \quad i_{sc}]^t$ and $\boldsymbol{\phi}_{sabc} = [\phi_{sa} \quad \phi_{sb} \quad \phi_{sc}]^t$ are the voltage, the current and the flux linkages of stator circuits respectively. $\boldsymbol{i}_{rabc} = [i_{ra} \quad i_{rb} \quad i_{rc}]^t$ and $\boldsymbol{\phi}_{rabc} = [\phi_{ra} \quad \phi_{rb} \quad \phi_{rc}]^t$ are the current and the flux linkages of rotor circuits respectively. $\mathbf{r}_s = diag[r_s \quad r_s \quad r_s]$ and $\mathbf{r}_r = diag[r_r \quad r_r \quad r_r]$ are the stator and rotor resistance matrices respectively.

$\mathbf{l}_s$, $\mathbf{l}_r$, and $\mathbf{m}_{\mathbf{sr}}(\theta)$ are the inductance matrices defined by:

$$\mathbf{l}_s = \begin{bmatrix} l_{ls}+l_{ms} & -\frac{l_{ms}}{2} & -\frac{l_{ms}}{2} \\ -\frac{l_{ms}}{2} & l_{ls}+l_{ms} & -\frac{l_{ms}}{2} \\ -\frac{l_{ms}}{2} & -\frac{l_{ms}}{2} & l_{ls}+l_{ms} \end{bmatrix} \quad \mathbf{l}_r = \begin{bmatrix} l_{lr}+l_{mr} & -\frac{l_{mr}}{2} & -\frac{l_{mr}}{2} \\ -\frac{l_{mr}}{2} & l_{lr}+l_{mr} & -\frac{l_{mr}}{2} \\ -\frac{l_{mr}}{2} & -\frac{l_{mr}}{2} & l_{lr}+l_{mr} \end{bmatrix}, \tag{3}$$

$$\mathbf{m}_{\mathbf{sr}}(\theta) = m \begin{bmatrix} \cos(\theta) & \cos\left(\theta+\frac{2\pi}{3}\right) & \cos\left(\theta+\frac{4\pi}{3}\right) \\ \cos\left(\theta+\frac{4\pi}{3}\right) & \cos(\theta) & \cos\left(\theta+\frac{2\pi}{3}\right) \\ \cos\left(\theta+\frac{2\pi}{3}\right) & \cos\left(\theta+\frac{4\pi}{3}\right) & \cos(\theta) \end{bmatrix}, \tag{4}$$

where r_s is stator phase resistance, r_r is rotor phase resistance, l_{ls} and l_{ms} are the leakage and the magnetizing inductance in the stator windings respectively, l_{lr} and l_{mr} are the leakage and the magnetizing inductance in the rotor windings respectively, m is the maximal mutual inductance between stator and rotor phase winding and θ is the electrical angle between the stator and the rotor phases.

The electromagnetic torque produced by the IM and the mechanical equations can be expressed as [1, 25]:

$$T_{em} = p\, \boldsymbol{i}_{sabc} \frac{\partial \mathbf{m}_{\mathbf{sr}}(\theta)}{\partial \theta} \boldsymbol{i}_{rabc}, \tag{5}$$

$$J\frac{d\,\Omega}{d\,t} = T_{em} - T_l - F\,\Omega. \tag{6}$$

Where p represents the number of pole pairs, Ω the mechanical angular velocity, J the moment of rotor inertia, F the viscose friction coefficient and T_l the load torque.

2.2. Machine equations in the stator fixed *dqo*-frame

To simplify the model of the IM described in *abc*-reference frame where the mutual inductance matrix (4) is function of electrical rotor position, it is necessary to use the variable transformation from *abc*-reference frame of the stator and the rotor variables to stator *dqo*-reference frame. This variable transformation is given by:

$$\boldsymbol{x}_{sdqo} = \boldsymbol{T}_{dqo}(\theta)\boldsymbol{x}_{sabc}, \quad \boldsymbol{x}_{rdqo} = \boldsymbol{T}_{dqo}(-\theta)\boldsymbol{x}_{rabc}. \tag{7}$$

Where subscript s and r denote the stator and the rotor variables respectively. The transformation matrix is given by:

$$\boldsymbol{T}_{dqo} = \frac{2}{3}\begin{bmatrix} \cos(\theta) & \cos(\theta - 2\pi/3) & \cos(\theta - 4\pi/3) \\ -\sin(\theta) & -\sin(\theta - 2\pi/3) & -\sin(\theta - 4\pi/3) \\ 1/2 & 1/2 & 1/2 \end{bmatrix}$$

On transforming (1) to the stationary reference frame, the voltage equations can be expressed as follows:

$$\begin{aligned} \boldsymbol{v}_{sdq} &= \mathbf{R}_s\,\boldsymbol{i}_{sdq} + \frac{d\boldsymbol{\phi}_{sdq}}{d\,t}, \\ v_{so} &= r_s\,i_{so} + \frac{d\phi_{so}}{d\,t}, \\ 0 &= \mathbf{R}_r\,\boldsymbol{i}_{rdq} + \frac{d\boldsymbol{\phi}_{rdq}}{d\,t} - p\Omega\,\mathbf{J}\boldsymbol{\phi}_{rdq}, \\ 0 &= r_r\,i_{ro} + \frac{d\phi_{ro}}{d\,t}. \end{aligned} \tag{8}$$

Where: x_{sdq} : *dq* transformed stator variables of the induction motor, i.e. $\boldsymbol{x}_{sdq} = (x_{sd}\;\; x_{sq})^t$, $\boldsymbol{x}_{rdq}$: *dq* transformed rotor variables of the induction motor, i.e. $\boldsymbol{x}_{rdq} = (x_{rd}\;\; x_{rq})^t$.

The stator and rotor flux linkages equations are given by:

$$\begin{aligned} \boldsymbol{\phi}_{sdq} &= \mathbf{L}_s\boldsymbol{i}_{sdq} + \mathbf{M}_{sr}\,\boldsymbol{i}_{rdq}, \\ \phi_{so} &= l_{ls}\,i_{so}, \\ \boldsymbol{\phi}_{rdq} &= \mathbf{L}_r\boldsymbol{i}_{rdq} + \mathbf{M}_{sr}\,\boldsymbol{i}_{sdq}, \\ \phi_{ro} &= l_{lr}\,i_{ro}. \end{aligned} \tag{9}$$

The parameter matrices $\mathbf{R}_s$, $\mathbf{R}_r$, $\mathbf{L}_s$, $\mathbf{L}_r$ and $\mathbf{M}_{sr}$ they all have a diagonal structure, and are given by,

$$\mathbf{R}_s = diag[r_s \;\; r_s], \mathbf{R}_r = diag[r_r \;\; r_r], \mathbf{L}_s = diag[l_s \;\; l_s], \mathbf{L}_r = diag[l_r \;\; l_r], \mathbf{M}_{sr} = diag[m_{sr} \;\; m_{sr}],$$

$$\mathbf{J} = \begin{bmatrix} 0 & -1 \\ 1 & 0 \end{bmatrix}.$$

With: $l_s = 3m/2 + l_{ls}$: stator cyclic inductance, $l_r = 3m/2 + l_{lr}$: rotor cyclic inductance, $m_{sr} = 3m/2$: stator-rotor cyclic mutual inductance.

Rewriting Equations (8) and (9), and using the magnetizing current $\boldsymbol{i}_{mdq}$ so defined that it fulfills the equation $\boldsymbol{\phi}_{rdq} = \mathbf{M}_{sr}\boldsymbol{i}_{mdq}$, the healthy induction motor model becomes:

$$\frac{d\boldsymbol{i}_{sdq}}{dt} = -\mathbf{L}_s^{'-1}\left(\mathbf{R}_s + \mathbf{R}_r^{'}\right)\boldsymbol{i}_{sdq} + \mathbf{L}_s^{'-1}\left(\mathbf{R}_r^{'} - p\Omega\,\mathbf{J}\,\mathbf{M}_{sr}^{'}\right)\boldsymbol{i}_{mdq} + \mathbf{L}_s^{'-1}\boldsymbol{v}_{sdq} \tag{10}$$

$$\frac{d\,i_{so}}{d\,t} = -\frac{r_s}{l_{ls}}i_{so} + \frac{1}{l_{ls}}v_{so}, \tag{11}$$

$$\frac{d\boldsymbol{i}_{mdq}}{dt} = \mathbf{M}_{sr}^{'-1}\mathbf{R}_r^{'}\,\boldsymbol{i}_{sdq} - \mathbf{M}_{sr}^{'-1}\left(\mathbf{R}_r^{'} - p\Omega\,\mathbf{J}\,\mathbf{M}_{sr}^{'}\right)\boldsymbol{i}_{mdq}, \tag{12}$$

$$\frac{d\,\phi_{ro}}{d\,t} = -\frac{r_r}{l_{lr}}\phi_{ro}. \tag{13}$$

Where $\mathbf{R}_r^{'} = \mathbf{M}_{sr}\,\mathbf{L}_r^{-1}\,\mathbf{R}_r\,\mathbf{L}_r^{-1}\,\mathbf{M}_{sr}$, $\mathbf{L}_s^{'} = \mathbf{L}_s - \mathbf{M}_{sr}\,\mathbf{L}_r^{-1}\,\mathbf{M}_{sr}$, $\mathbf{M}_{sr}^{'} = \mathbf{M}_{sr}\,\mathbf{L}_r^{-1}\,\mathbf{M}_{sr}$. From equation of ϕ_{ro}, it is seen that the flux components $\phi_{ro} = 0$ when $t \to \infty$, for every possible operating conditions, therefore this Equation (14) can be excluded from the final IM model.

For the case of the isolated star point of winding circuit, the sums of the three stator and rotor phase currents are zero i.e.: $i_{sa} + i_{sb} + i_{sc} = 0$ and $i_{ra} + i_{rb} + i_{rc} = 0$. Therefore the homopolar component $i_{so} = 0$ and $i_{ro} = 0$ and the equation of the homopolar variables described by (11) becomes: $v_{so} = 0$. This shows that Equation (11) has no effect on the IM behavior and can be excluded from finally model.

By application of variables transformations given by (7) to the torque expression (5) and using the magnetizing currents expression $\boldsymbol{i}_{mdq} = (l_r/m_{sr})\boldsymbol{i}_{rdq} + \boldsymbol{i}_{sdq}$ the following torque expression is obtained:

$$T_{em} = \frac{3}{2}p\frac{m_{sr}^2}{l_r}\left(i_{md}i_{sq} - i_{mq}i_{sd}\right). \tag{14}$$

3. Induction motor model with stator fault

3.1. Machine equations in abc variables

The scheme of a wye-connected three phase stator windings with a short circuit between turns of the phase '*a*' winding is shown in Figure 1, where the machine with a fault can be modeled as if the stator had four different windings i.e. 'as_1', 'as_2', 'bs' and 'cs'. The windings 'as_1' and 'as_2' represent the healthy and shorted turns respectively and the current 'i_f' represents the circulating current in the shorted turns. The fraction of shorted turns γ_a is defined as the ration of the number of the shorted turns to the turns per phase. In The model presented below, it is assumed that the leakage inductance and the resistance of shorted winding are proportional to the fraction of shorted turns 'γ_a'.

In this section a model of an induction motor, including an inter-turn short circuit in phase 'a', is developed. The model is developed under the assumption that the short circuit does not affect the overall angular position of the coil in the motor.

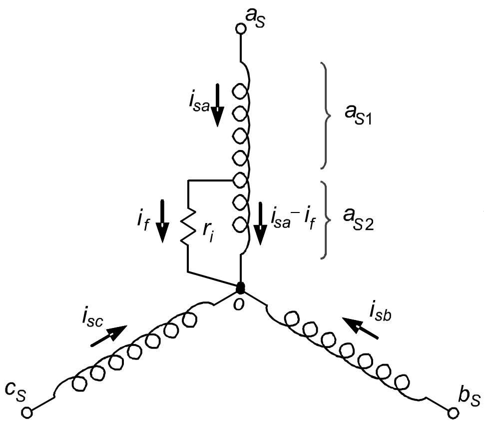

Fig. 1. Scheme of three phase stator winding with a short circuit between turns of phase 'a'

Using the matrix notation, the equations of the stator and rotor voltages and flux and produced torque with stator turns fault can be expressed as follows [26-28]:

$$\boldsymbol{v}'_{sabc} = \boldsymbol{r}'_s \, \boldsymbol{i}'_{sabc} + \frac{d\boldsymbol{\phi}'_{sabc}}{d\,t}, \tag{15}$$

$$\mathbf{0} = \boldsymbol{r}_r \, \boldsymbol{i}_{rabc} + \frac{d\boldsymbol{\phi}_{rabc}}{d\,t}, \tag{16}$$

$$\boldsymbol{\phi}'_{sabc} = \mathbf{l}'_s \, \boldsymbol{i}'_{sabc} + \mathbf{m}'_{\mathrm{sr}}(\theta)\, \boldsymbol{i}_{rabc}, \tag{17}$$

$$\boldsymbol{\phi}_{rabc} = \mathbf{l}_r \, \boldsymbol{i}_{rabc} + \mathbf{m}'^{t}_{\mathrm{sr}}(\theta)\, \boldsymbol{i}'_{sabc}, \tag{18}$$

$$T_{em} = \boldsymbol{i}'^{t}_{sabc} \frac{\partial \boldsymbol{m}'_{sr}(\theta)}{\partial\theta} \boldsymbol{i}_{rabc}. \tag{19}$$

Where $\boldsymbol{v}'_{sabc} = [v_{sa1}\ v_{sa2}\ v_{sb}\ v_{sc}]^t$, $\boldsymbol{i}'_{sabc} = [i_{sa}\ i_{sa} - i_f\ i_{sb}\ i_{sc}]^t$, $\boldsymbol{\phi}'_{sabc} = [\phi_{sa1}\ \phi_{sa2}\ \phi_{sb}\ \phi_{sc}]^t$.

The resistance and the self inductance matrices of rotor winding are not affected by fault and are of the same form as in Section 2-1. The resistance, the self inductance matrices of stator winding and the mutual inductance change under an influence of the inter-turn stator fault in phase 'a' condition which can be represented as follows:

$$\boldsymbol{r}_s' = diag\left[(1-\gamma_a)r_s\ \gamma_a r_s\ r_s\ r_s\right],$$

$$\mathbf{l}_s' = \begin{bmatrix} (1-\gamma_a)l_{ls} + (1-\gamma_a)^2 l_{ms} & \gamma_a(1-\gamma_a)l_{ms} & -(1-\gamma_a)l_{ms}/2 & -(1-\gamma_a)l_{ms}/2 \\ \gamma_a(1-\gamma_a)l_{ms} & \gamma_a l_{ls} + \gamma_a^2 l_{ms} & -\gamma_a l_{ms}/2 & -\gamma_a l_{ms}/2 \\ -(1-\gamma_a)l_{ms}/2 & -\gamma_a l_{ms}/2 & l_{ls} + l_{ms} & -l_{ms}/2 \\ -(1-\gamma_a)l_{ms}/2 & -\gamma_a l_{ms}/2 & -l_{ms}/2 & l_{ls} + l_{ms} \end{bmatrix}$$

$$\mathbf{m}_{sr}'(\theta) = m \begin{bmatrix} (1-\gamma_a)\cos(\theta) & (1-\gamma_a)\cos(\theta + \frac{2\pi}{3}) & (1-\gamma_a)\cos(\theta + \frac{4\pi}{3}) \\ \gamma_a \cos(\theta) & \gamma_a \cos(\theta + \frac{2\pi}{3}) & \gamma_a \cos(\theta + \frac{4\pi}{3}) \\ \cos\left(\theta + \frac{4\pi}{3}\right) & \cos(\theta) & \cos(\theta + \frac{2\pi}{3}) \\ \cos\left(\theta + \frac{2\pi}{3}\right) & \cos(\theta + \frac{4\pi}{3}) & \cos(\theta) \end{bmatrix}$$

On adding the first two rows of the matrix Equation (15), rearranging terms and noting that $\boldsymbol{v}_{sa} = v_{sa1} + v_{sa2}$, the voltage equations can be written as follows:

$$\begin{aligned} \boldsymbol{v}_{sabc} &= \boldsymbol{r}_s \left(\boldsymbol{i}_{sabc} - \begin{bmatrix} \gamma_a \\ 0 \\ 0 \end{bmatrix} i_f \right) + \frac{d\boldsymbol{\phi}_{sabc}}{dt}, \\ \mathbf{0} &= \boldsymbol{r}_r\, \boldsymbol{i}_{rabc} + \frac{d\boldsymbol{\phi}_{rabc}}{dt}. \end{aligned} \tag{20}$$

Where the rotor and stator flux equations can be written respectively as follows:

$$\begin{aligned} \boldsymbol{\phi}_{sabc} &= \mathbf{l}_s \left(\boldsymbol{i}_{sabc} - \begin{bmatrix} \gamma_a \\ 0 \\ 0 \end{bmatrix} i_f \right) + \mathbf{m_{sr}}(\theta)\, \boldsymbol{i}_{rabc}, \\ \boldsymbol{\phi}_{rabc} &= \mathbf{l}_r \boldsymbol{i}_{rabc} + \mathbf{m_{sr}}(\theta) \left(\boldsymbol{i}_{sabc} - \begin{bmatrix} \gamma_a \\ 0 \\ 0 \end{bmatrix} i_f \right). \end{aligned} \tag{21}$$

The expressions for the voltages at the healthy turns (as_1) and the shorted turns (as_2) in the winding of phase 'a' can be obtained from Equations (15) and (17), respectively as:

$$\boldsymbol{v}_{sa1} = (1-\gamma_a)\left[r_s\, i_{sa} + \mathbf{A}_1 \frac{d\boldsymbol{i}_{sabc}}{dt} + \frac{d\{\mathbf{A}_2(\theta)\cdot \boldsymbol{i}_{sabc}\}}{dt} \right] - \gamma_a(1-\gamma_a) l_{ms} \frac{di_f}{dt}, \tag{22}$$

$$\boldsymbol{v}_{sa2} = r_i i_f = \gamma_a \left[r_s\, i_{sa} + \mathbf{A}_1 \frac{d\boldsymbol{i}_{sabc}}{d\,t} + \frac{d\left\{\mathbf{A}_2(\theta)\cdot \boldsymbol{i}_{sabc}\right\}}{d\,t}\right] - \gamma_a r_s i_f - \gamma_a\left(l_{ls} + \gamma_a l_{ms}\right)\frac{di_f}{d\,t}, \quad (23)$$

Where $\mathbf{A}_1 = [l_{ls} + l_{ms}\ \ -l_{ms}/2\ \ -l_{ms}/2]$, $\mathbf{A}_2(\theta) = m[\cos(\theta)\ \cos(\theta + 2\pi/3)\ \cos(\theta + 4\pi/3)]$. By manipulations on the equation (22) and (23) and by considering that the voltages v_{sa1} and v_{sa2} are proportional to $(1 - \gamma_a)$ and γ_a respectively, the equation describing the current in the short circuit can be obtained by:

$$[\gamma_a\ 0\ 0]\boldsymbol{v}_{sabc} = r_f i_f + l_f \frac{di_f}{d\,t}. \quad (24)$$

The inductance and the resistance of the short circuit are given by wrong

$$l_f = \gamma_a\left(1-\gamma_a\right)l_{ls}, \quad r_f = \gamma_a\left(1-\gamma_a\right)r_s + r_i.$$

Where r_i is the resistance in the insulation break. $r_i = \infty$ means that no short circuit has occurred and $r_i \neq \infty$ means that some leakage current is flowing.

On rearranging terms in (19), the torque developed by the machine can be expressed as:

$$T_{em} = \left\{\left[\left(1-\gamma_a\right)i_{sa}\ i_{sb}\ i_{sc}\right]\frac{\partial \mathbf{m}_{sr}(\theta)}{\partial\theta} + \gamma_a\left(i_{sa} - i_f\right)\frac{\partial A_3(\theta)}{\partial\theta}\right\}\boldsymbol{i}_{rabc} =$$
$$= \left(\boldsymbol{i}_{sabc} - \begin{bmatrix}\gamma_a\\ 0\\ 0\end{bmatrix}\partial_{i_f}\right)^t \frac{\mathbf{m}_{sr}(\theta)}{\partial\theta}\boldsymbol{i}_{rabc}. \quad (25)$$

3.2. Faulty model in the stator fixed *dqo*-frame

In this section, the model of IM with short circuit in the phase '*a*' in the stationary reference frame is developed. The application of transformation given by (7) on the vector current $(\boldsymbol{i}_{sabc} - [\gamma_a\ 0\ 0]^t i_f)$ gives $(\boldsymbol{i}'_{sdqo} = (\boldsymbol{i}_{sdqo} - T_{dqo}[\gamma_a\ 0\ 0]^t i_f))$.

The model described in Section 3-1 transformed to the stationary reference frame gives the following equations, with making use of the new defined current vector:

$$\boldsymbol{v}_{sdqo} = \mathbf{R}_s\,\boldsymbol{i}'_{sdq} + \frac{d\boldsymbol{\phi}_{sdq}}{d\,t},$$
$$0 = \mathbf{R}_r\,\boldsymbol{i}_{rdq} + \frac{d\boldsymbol{\phi}_{rdq}}{d\,t} - p\Omega\,\mathbf{J}\boldsymbol{\phi}_{rdq}, \quad (26)$$

$$v_{so} = r_s\, i'_{so} + \frac{d\phi_{so}}{d\,t}, \quad (27)$$

$$0 = r_r\,\boldsymbol{i}_{ro} + \frac{d\phi_{ro}}{d\,t}, \quad (28)$$

$$[\gamma_a \ 0 \ 0]\mathbf{T}_{dqo}^{-1}\boldsymbol{v}_{sdqo} = r_f i_f + l_f \frac{di_f}{dt}, \tag{29}$$

$$\begin{aligned} \boldsymbol{\phi}_{sdq} &= \mathbf{L}_s \, \boldsymbol{i}'_{sdq} + \mathbf{M}_{sr} \, \boldsymbol{i}_{rdq}, \\ \boldsymbol{\phi}_{rdq} &= \mathbf{L}_r \, \boldsymbol{i}_{rdq} + \mathbf{M}_{sr} \, \boldsymbol{i}'_{sdq}, \end{aligned} \tag{30}$$

$$\phi_{so} = l_{ls} \, i'_{so}, \tag{31}$$

$$\phi_{ro} = l_{lr} \, i_{ro}. \tag{32}$$

Where:

$$(\boldsymbol{i}'_{sdq} = (\boldsymbol{i}_{sdq} - \boldsymbol{T}_{dq}[\gamma_a \ 0 \ 0]^t i_f), \tag{33}$$

$$i'_{so} = i_{so} - \frac{1}{3}\gamma_a i_f, \tag{34}$$

$$\mathbf{T}_{dq} = \frac{2}{3}\begin{bmatrix} 1 & -1/2 & -1/2 \\ 0 & \sqrt{3/2} & -\sqrt{3/2} \end{bmatrix}. \tag{35}$$

By substituting Equation (33) into (28), the expression of the flux ϕ_{ro} is obtained as follows:

$$\frac{d\phi_{ro}}{dt} + \frac{r_r}{l_{lr}}\phi_{ro} = 0. \tag{36}$$

This equation can be excluded from the final model because $\phi_{ro} \to 0$ when $t \to \infty$.

The last row of voltage $\boldsymbol{v}_{sdqo}$ in Equation (29), equals v_{so}, is unknown, and it is necessary to calculate the short circuit current, as indicate by (29). Since the homopolar component of stator current $i_{so} = 0$ in a Y-connected motor winding, from Equations (34), (31) and (27), we can obtain the following expression:

$$v_{so} = -\frac{1}{3}\gamma_a r_s i_f - \frac{1}{3}\gamma_a l_{ls}\frac{di_f}{dt}. \tag{37}$$

Including the expression (37) of v_{so} in (29), the dynamic equation of the short circuit current is expressed as:

$$\gamma_a v_{sd} = R_f i_f + L_f \frac{di_f}{dt}, \tag{38}$$

where $L_f = l_f + \gamma_a^2 l_{ls}/3$ and $R_f = r_f + \gamma_a^2 r_s/3$.

The final Equations describing the electrical part of IM are given by (26), (30) and (38). Rewriting these equations with introducing the stator current $\boldsymbol{i}'_{sdq}$ and magnetizing current $\boldsymbol{i}_{mdq}$, the IM model in case of inter-turn short circuit becomes:

$$\begin{gathered}\frac{d\boldsymbol{i}'_{sdq}}{dt} = -\mathbf{L}_s^{'-1}\left(\mathbf{R}_s + \mathbf{R}_r^{'}\right)\boldsymbol{i}'_{sdq} + \mathbf{L}_s^{'-1}\left(\mathbf{R}_r^{'} - p\,\Omega\,\mathbf{J}\,\mathbf{M}_{sr}^{'}\right)\boldsymbol{i}_{mdq} + \mathbf{L}_s^{'-1}\boldsymbol{v}_{sdq}, \\ \frac{d\boldsymbol{i}_{sdq}}{dt} = \mathbf{M}_{sr}^{'-1}\mathbf{R}_r^{'}\boldsymbol{i}'_{sdq} - \mathbf{M}_{sr}^{'-1}\left(\mathbf{R}_r^{'} - p\,\Omega\,\mathbf{J}\,\mathbf{M}_{sr}^{'}\right)\boldsymbol{i}_{mdq}, \\ \frac{di_f}{dt} = -\frac{R_f}{L_f}i_f + \frac{\gamma_a}{L_f}v_{sd}.\end{gathered} \tag{39}$$

Where the new matrices used, retaining the diagonal structure, are given by:

$$\mathbf{R}_r^{'} = \mathbf{M}_{sr}\,\mathbf{L}_r^{-1}\,\mathbf{R}_r\,\mathbf{L}_r^{-1}\,\mathbf{M}_{sr},\quad \mathbf{L}_s^{'} = \mathbf{L}_s - \mathbf{M}_{sr}\,\mathbf{L}_r^{-1}\,\mathbf{M}_{sr},\quad \mathbf{M}_{sr}^{'} = \mathbf{M}_{sr}\,\mathbf{L}_r^{-1}\,\mathbf{M}_{sr}.$$

Transforming the torque expression given by (25) by variables transformations (7), the following final torque expression is obtained:

$$T_{em} = \frac{3}{2}\,p\,\frac{m_{sr}^2}{l_r}\left(i_{md}i'_{sq} - i_{mq}i'_{sd}\right). \tag{40}$$

The final model describing the electrical and the electromechanical parts of IM is given by Equations (39), (40) and (6). It is used to the numerical simulation of the IM with inter-turn short-circuit fault in stator phase '*a*'.

4. Observer for short circuit fault detection

The main objective of this part was to establish the online system to be capable of detecting the short circuit stator condition in IM. We propose the use of an observer based on the bilinear model of the IM operating with inter-turn short circuit fault in order to estimate the fraction of short circuit turns and other IM states such as presented in the following. This section ends with presenting the design procedure for this observer.

The state space model version of the induction motor equations with inter-turn short circuit in the phase '*a*' developed in Section 3.2 by Eq. (39) can be written as the following system:

$$\begin{gathered}\dot{\boldsymbol{x}} = \left(\mathbf{A}_0 + \Omega\mathbf{A}_\Omega\right)\boldsymbol{x} + \mathbf{B}\boldsymbol{u} \\ \boldsymbol{y} = \mathbf{C}\,\boldsymbol{x},\end{gathered} \tag{41}$$

where $\boldsymbol{x} = [\boldsymbol{i}'^{t}_{sdq}\ \boldsymbol{i}^{t}_{mdq}\ i_f]^t$, $\boldsymbol{u} = \boldsymbol{v}_{sdq}$, $y = \boldsymbol{i}_{sdq}$.

The matrices used in this model are given by:

$$\mathbf{A}_0 = \begin{bmatrix} -\mathbf{L}_s^{'-1}\left(\mathbf{R}_s + \mathbf{R}_r^{'}\right) & \mathbf{L}_s^{'-1}\mathbf{R}_r^{'} & \mathbf{0} \\ \mathbf{M}_{sr}^{'-1}\mathbf{R}_r^{'} & -\mathbf{M}_{sr}^{'-1}\mathbf{R}_r^{'} & \mathbf{0} \\ \mathbf{0} & \mathbf{0} & -R_f/L_f \end{bmatrix},\quad \mathbf{A}_\Omega = \begin{bmatrix} \mathbf{0} & -p\mathbf{J}\mathbf{M}'_{sr} & 0 \\ \mathbf{0} & -p\,\mathbf{J} & 0 \\ \mathbf{0} & \mathbf{0} & 0 \end{bmatrix},$$

$$\mathbf{B} = \begin{bmatrix} -\mathbf{L}_s^{'-1} \\ \mathbf{0} \\ [\gamma_a / L_f\ \ 0] \end{bmatrix},\quad \mathbf{C} = \begin{bmatrix} \mathbf{I} & \mathbf{0} & \mathbf{T}_{dq}\begin{bmatrix}\gamma_a \\ 0 \\ 0\end{bmatrix} \end{bmatrix},\quad \mathbf{I} = \begin{bmatrix} 1 & 0 \\ 0 & 1 \end{bmatrix}.$$

In order that the fault coefficient appears in the fault detection observer, let us define a transformation $\boldsymbol{x} = \mathbf{T}_{zx}\boldsymbol{z}$. This transformation gives the bilinear version of the non-linear system (41), where the transformation matrix is given by:

$$\mathbf{T}_{zx} = \begin{bmatrix} \mathbf{I} & \mathbf{0} & [-1\ 0]^t \\ -\mathbf{M}'^{-1}_{sr}\mathbf{L}'_s & \mathbf{I} & \mathbf{0} \\ \mathbf{0} & \mathbf{0} & 3/2\gamma_a \end{bmatrix}. \tag{42}$$

When this transformation is used on system (6) it gives the following bilinear system:

$$\begin{aligned} \dot{\boldsymbol{z}} &= \left(\mathbf{A}_{z0} + \Omega\mathbf{A}_{z\Omega} + v_{sd} + \mathbf{A}_{zv_{sd}}\right)\boldsymbol{z} + \mathbf{B}_z\boldsymbol{u} \\ \boldsymbol{y}_z &= \mathbf{C}_z\,\boldsymbol{z}. \end{aligned} \tag{43}$$

The new state vector $\boldsymbol{z}$ is extended by another variable describing the fault characteristic, where $\boldsymbol{z} = [\mathbf{T}_{zx}^{-1}\boldsymbol{x}\ f]$. f represent the fault characteristic and is defined as:

$$f = \frac{\gamma_a}{\left(1 - \frac{2}{3}\gamma_a\right)}. \tag{44}$$

In system (43), the input and the output vectors are: $\boldsymbol{u} = \boldsymbol{v}_{sdq}$, $\boldsymbol{y}_z = \boldsymbol{i}_{sdq}$ and the matrices are:

$$\mathbf{A}_{z0} = \begin{bmatrix} (-\mathbf{L}'^{-1}_s(\mathbf{R}_s + \mathbf{R}'_r) - \mathbf{M}'^{-1}_{sr}\mathbf{R}'_r) & -\mathbf{L}'^{-1}_s\mathbf{R}'_r & (\mathbf{L}'^{-1}_s(\mathbf{R}_s + \mathbf{R}'_r)\begin{bmatrix}1\\0\end{bmatrix} - \begin{bmatrix} r_s/l_{ls} \\ 0\end{bmatrix} & \mathbf{0} \\ -\mathbf{M}'^{-1}_{sr}\mathbf{R}'_r & \mathbf{0} & (\mathbf{M}'^{-1}_{sr}(\mathbf{R}_s - \frac{r_s}{l_{ls}}\mathbf{L}'_s)\begin{bmatrix}1\\0\end{bmatrix} & \mathbf{0} \\ \mathbf{0} & \mathbf{0} & -r_s/l_{ls} & 0 \\ \mathbf{0} & \mathbf{0} & 0 & 0 \end{bmatrix},$$

$$\mathbf{A}_{z\Omega} = \begin{bmatrix} pJ & -pJ\mathbf{L}'^{-1}_s\mathbf{M}'_{sr} & \mathbf{0} & \mathbf{0} \\ \mathbf{0} & \mathbf{0} & \mathbf{0} & \mathbf{0} \\ \mathbf{0} & \mathbf{0} & 0 & 0 \\ \mathbf{0} & \mathbf{0} & 0 & 0 \end{bmatrix}, \quad \mathbf{A}_{zv_{zd}} = \begin{bmatrix} \mathbf{0} & \mathbf{0} & \mathbf{0} & \begin{bmatrix} 2/3l_{ls} \\ 0 \end{bmatrix} \\ \mathbf{0} & \mathbf{0} & \mathbf{0} & \left((2/3l_{ls})\mathbf{M}'^{-1}_{sr}\mathbf{L}'_s\begin{bmatrix}1\\0\end{bmatrix}\right) \\ \mathbf{0} & \mathbf{0} & 0 & 2/3l_{ls} \\ \mathbf{0} & \mathbf{0} & 0 & 0 \end{bmatrix},$$

$$\mathbf{B}_z = \begin{bmatrix} \mathbf{L}'^{-1}_s \\ \mathbf{M}'^{-1}_{sr} \\ \mathbf{0} \\ \mathbf{0} \end{bmatrix}, \quad \mathbf{C}_z = [\mathbf{I}\quad \mathbf{0}\quad 0\quad 0].$$

The observer based on the bilinear system defined by (43) has the following form:

$$\begin{aligned}\dot{\hat{z}} &= \mathbf{A}_z(\Omega,\ v_{sd})\hat{z} + \mathbf{B}_z \boldsymbol{u} + \mathbf{K}(v_{sd})(\boldsymbol{y}_z - \hat{\boldsymbol{y}}_z) \\ \hat{\boldsymbol{y}}_z &= \mathbf{C}_z\ \hat{z},\end{aligned} \tag{45}$$

where ^ means the estimated value and the estimated output, $\mathbf{K}(v_{sd})$ is the stabilizing feedback gain of observer and the matrix $\mathbf{A}_z(\Omega,\ v_{sd})$ is defined as:

$$\mathbf{A}_z(\Omega,\ v_{sd}) = \mathbf{A}_{z0} + \Omega\mathbf{A}_{z\Omega} + v_{sd}\mathbf{A}_{zv_{sd}}.$$

For a design of this observer, we define the state estimation error as:

$$\boldsymbol{e}_z = z - \hat{z}.$$

The dynamic of the estimated error is described by the following equation:

$$\frac{d\boldsymbol{e}_z}{dt} = \left[\mathbf{A}_z(\Omega,\ v_{sd}) - \mathbf{K}(v_{sd})\mathbf{C}_z\right]\boldsymbol{e}_z. \tag{46}$$

The results can be formulated as in the following.

Proposition 1

Consider observer given by (45), assume that Ω has slow dynamics with respect to voltage v_{sd}. Let, the observer gain matrix be

$$\mathbf{K}(v_{sd}) = \mathbf{K}_0 + \mathbf{K}_1 v_{sd}, \tag{47}$$

Where gains $\mathbf{K}_0$ and $\mathbf{K}_1$ are such that the matrix $\mathbf{A}_z(\Omega,\ v_{sd}) - \mathbf{K}(v_{sd})\mathbf{C}_z$ is negative definite. Then, the observation error $\boldsymbol{e}_z = z - \hat{z}$ is asymptotically stable.

Proof

The stability of the observation error can be proved by Lyapunov stability theory. Choosing a Lyapunov candidate function as: $V = \boldsymbol{e}_z^T \boldsymbol{e}_z / 2$.

The Lyapunov function is positive definite, what satisfies the stability first condition. Its time-derivative is expressed by: $\dot{V} = \boldsymbol{e}_z^T \dot{\boldsymbol{e}}_z$.

To satisfy the Lyapunov stability, second condition must satisfy $\dot{V} < 0$. From Equation (46), we can write:

$$\dot{V} = \boldsymbol{e}_z^T\left[\mathbf{A}_z(\Omega,\ v_{sd}) - \mathbf{K}(v_{sd})\mathbf{C}_z\right]\boldsymbol{e}_z < 0. \tag{48}$$

what means that the matrix:

$$\left[\mathbf{A}_z(\Omega,\ v_{sd}) - \mathbf{K}(v_{sd})\mathbf{C}_z\right] < 0 \tag{49}$$

must be negative definite.

From expression of $\mathbf{A}_z(\Omega,\ v_{sd})$, given in (43), and Equation (47), the Equation (49) can be rewritten as:

$$(\mathbf{A}_{z0} - \mathbf{K}_0\mathbf{C}_z) + \Omega\mathbf{A}_{z\Omega} + v_{sd}\left(\mathbf{A}_{zv_{sd}} - \mathbf{K}_1\mathbf{C}_z\right).$$

In order to avoid the effect of the variation of the voltage v_{sd} on the dynamics of the observer, $\mathbf{K}_1$ can be chosen so that the eigenvalues of the matrix $\left(\mathbf{A}_{zv_{sd}} - \mathbf{K}_1\mathbf{C}_z\right)$ are located on the imaginary axis.

5. Fault tolerant control based field oriented control

In this section, we propose a FTC based on the IRFOC and the observer developed in Section 4 in order to maintain the decoupling between rotor flux control and developed torque control of IM. For the current controllers inputs, the FTC switches between the $\boldsymbol{i}_{sdq}^{(e)}$ measured $d-q$ axis components of stator current in the case of the absence of short circuit fault, and the $\hat{\boldsymbol{i}}'^{(e)}_{sdq}$ estimated $d-q$ axis components of stator current when the short circuit fault occurs.

The electrical dynamic model of IM in case of healthy condition in the synchronously rotating reference frame, where the $d-q$ axis components of stator and magnetizing currents are considered as state variables, can be expressed as [1, 23]:

$$v_{sd}^{(e)} = \sigma l_s \frac{di_{sd}^{(e)}}{dt} + \left(r_s + r_r \frac{m_{sr}^2}{l_r^2}\right) i_{sd}^{(e)} - \omega_s \sigma l_s i_{sd}^{(e)} - \frac{m_{sr}^2}{l_r^2} r_r i_{sd}^{(e)} - \frac{m_{sr}^2}{l_r^2} \omega i_{mq}^{(e)}, \tag{50}$$

$$v_{sd}^{(e)} = \sigma l_s \frac{di_{sq}^{(e)}}{dt} + \left(r_s + r_r \frac{m_{sr}^2}{l_r^2}\right) i_{sq}^{(e)} - \omega_s \sigma l_s i_{sd}^{(e)} + \frac{m_{sr}^2}{l_r} \omega i_{md}^{(e)} - \frac{m_{sr}^2}{l_r^2} r_r i_{mq}^{(e)}, \tag{51}$$

$$0 = \frac{r_r}{l_r} i_{sd}^{(e)} + \frac{di_{md}^{(e)}}{dt} + \frac{r_r}{l_r} i_{md}^{(e)} - \omega_r i_{mq}^{(e)}, \tag{52}$$

$$0 = -\frac{r_r}{l_r} i_{sq}^{(e)} + \frac{di_{mq}^{(e)}}{dt} + \frac{r_r}{l_r} i_{mq}^{(e)} + \omega_r i_{md}^{(e)}. \tag{53}$$

The superscript $^{(e)}$, designates a variable in the synchronous rotating frame, where $\sigma = 1 - m_{sr}^2/(l_s l_r)$ is the leakage coefficient, $\omega = p\Omega$ is the electrical speed of the rotor, ω_s is the electrical synchronously rotating speed and $\omega_r = \omega_s - \omega$ is the slip electrical rotor speed.

The electromagnetic torque generated by the IM in case of healthy condition given by (14), is valid for synchronously rotating reference frame and may be expressed as:

$$T_{em} = \frac{3}{2} p \frac{m_{sr}}{l_r}\left(\phi_{rd}^{(e)} i_{sq}^{(e)} - \phi_{rq}^{(e)} i_{sd}^{(e)}\right) = \frac{3}{2} p \frac{m_{sr}^2}{l_r}\left(i_{md}^{(e)} i_{sq}^{(e)} - i_{mq}^{(e)} i_{sd}^{(e)}\right). \tag{54}$$

The relations between the $d-q$ axis components of rotor flux and those of magnetizing rotor current in the synchronously rotating reference frame are given by the following expressions:

$$\phi_{rd}^{(e)} = m_{sr} i_{md}^{(e)}, \; \phi_{rq}^{(e)} = m_{sr} i_{mq}^{(e)}. \tag{55}$$

For rotor field oriented control [1, 2], the instantaneous speed of the rotor flux vector is selected to revolve at synchronous speed and the d-axis of reference frame is aligned to the rotor flux direction as shown in Fig. 2 . The q-axis components of rotor flux vanishes and the rotor flux is entirely in the d-axis, i.e.,

$$\phi_{rd}^{(e)} = \phi_r \ \text{ and } \ \phi_{rq}^{(e)} = \dot{\phi}_{rq}^{(e)} = 0, \tag{56}$$

where ϕ_r denote the rotor flux and the components of magnetizing current become:

$$i_{md}^{(e)} = i_m^{(e)} \quad \text{and} \quad i_{mq}^{(e)} = 0. \tag{57}$$

Substituting Equations (57) into Equations (50) to (53) and (54) yields:

$$v_{sd}^{(e)} = \sigma l_s \frac{di_{sd}^{(e)}}{dt} + \left(r_s + r_r \frac{m_{sr}^2}{l_r^2} \right) i_{sd}^{(e)} - \omega_s \sigma l_s i_{sq}^{(e)} - \frac{m_{sr}^2}{l_r^2} r_r i_m^{(e)}, \tag{58}$$

$$v_{sq}^{(e)} = \sigma l_s \frac{di_{sq}^{(e)}}{dt} + \left(r_s + r_r \frac{m_{sr}^2}{l_r^2} \right) i_{sq}^{(e)} - \omega_s \sigma l_s i_{sd}^{(e)} + \frac{m_{sr}^2}{l_r} \omega i_m^{(e)}, \tag{59}$$

$$0 = -\frac{r_r}{l_r} i_{sd}^{(e)} + \frac{di_{md}^{(e)}}{dt} + \frac{r_r}{l_r} i_m^{(e)}, \tag{60}$$

$$0 = -\frac{r_r}{l_r} i_{sq}^{(e)} + \frac{di_{mq}^{(e)}}{dt} + \omega_r i_{md}^{(e)}. \tag{61}$$

$$T_{em} = \frac{3}{2} p \frac{m_{sr}}{l_r} \phi_r^{(e)} i_{sq}^{(e)} = \frac{3}{2} p \frac{m_{sr}^2}{l_r} i_m^{(e)} i_{sq}^{(e)}. \tag{62}$$

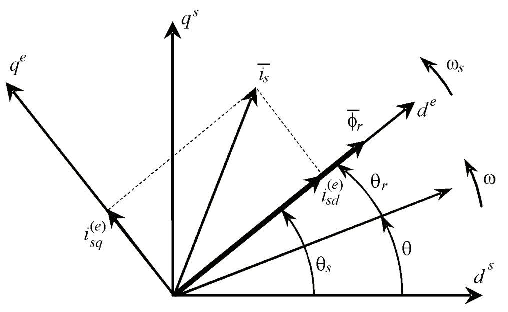

Fig. 2. Phasor diagram explaining IRFOC

The Equation (62) indicates that if the rotor flux ϕ_r ($i_m^{(e)}$) is constant for a constant torque operation, the electromagnetic torque T_{em} can be linearly varied by adjusting $i_{sq}^{(e)}$ current.

Therefore, a field-oriented control method controls the IM as if it was a separately excited DC machine.

In the case of indirect rotor flux control, the required *d*-axis component of the stator current $i_{sd}^{(e)*}$, to achieve a demanded rotor flux magnitude ϕ_r^* $(i_m^{(e)*})$, can be determined from Eq. (60).

The required q-axis component of the stator current, $i_{sq}^{*(e)}$, for a given torque demand T_{em}^*, can be determined from equation (62).

The necessary rotor flux angle θ_s^*, required to transform between the stationary and rotating reference frame quantities, is computed as follows:

$$\theta_s^* = \int \omega_s^* dt, \tag{63}$$

where $\omega_s^* = \omega_r^* + \omega$ is the command rotor flux speed. The command slip speed is obtained from equation (61) as follow:

$$\omega_r^* = \frac{1}{\tau_r \, i_{sd}^{*(e)}} i_{sq}^{*(e)}. \tag{64}$$

Let $R(\theta_s)$ be the transformation matrix between stator fixed and field rotating reference frame. It is given by:

$$R(\theta_s) = \begin{bmatrix} \cos(\theta_s) & \sin(\theta_s) \\ -\sin(\theta_s) & \cos(\theta_s) \end{bmatrix}.$$

The results can be formulated as in the following.

Proposition 2

Let $i_{sd}'^{(e)}$ and $i_{sq}'^{(e)}$ be the components of estimated stator current, in the field rotating reference frame produced by observer developed in Proposition 1, and let:

$$\hat{\boldsymbol{i}}'_{sdq} = \begin{bmatrix} \mathbf{I} & \mathbf{0} & [-1\,0]^t \end{bmatrix} \hat{z} \quad \text{and} \quad \hat{i}_{sdq}'^{(e)} = R(\theta_s)\hat{\boldsymbol{i}}'_{sdq}. \tag{65}$$

Then, decoupling between the torque and rotor flux controls is maintained also in the presence of inter-turn short circuit.

Proof

In the case of inter-turn short circuit fault condition, the torque expression given by Equation (40), which it is valid for all reference frames, can be expressed as

$$T_{em} = \frac{3}{2} p \frac{m_{sr}^2}{l_r} \left(i_{md}^{(e)} i_{sq}'^{(e)} - i_{mq}^{(e)} i_{sd}'^{(e)} \right). \tag{66}$$

From Equation (30), the expression of rotor flux can be also written in synchronously rotating reference frame as:

$$\phi_{rdq}^{(e)} = \mathbf{L}_r \boldsymbol{i}_{rdq}^{(e)} + \mathbf{M}_{sr} \boldsymbol{i}_{rdq}'^{(e)}. \tag{67}$$

After the orientation of the rotor flux vector along the d-axis and using the torque and rotor flux expressions (66) and (67) respectively, we obtain:

$$T_{em} = \frac{3}{2} p \frac{m_{sr}^2}{l_r} i_{md}^{(e)} i'^{(e)}_{sq}, \tag{68}$$

$$\phi_{rd}^{(e)} = \frac{m_{sr}}{1+\tau_r s} i'^{(e)}_{sd}, \quad i_{md}^{(e)} = \frac{1}{1+\tau_r s} i'^{(e)}_{sd}. \tag{69}$$

In inter-turn short circuit failure conditions, to maintain the decoupling between the torque and rotor flux controls, it is necessary to control the estimated $d-q$ axis components of stator currents '$\boldsymbol{i}'^{(e)}_{sdq}$' in the synchronously rotating reference frame like it is defined by the expressions (68) and (69).

The estimated $d-q$ axis components of stator current '$\hat{\boldsymbol{i}}'^{(e)}_{sdq}$' can be obtained after coordinates transformation from estimated states given by observer defined in Section 4 with the transformation matrices defined by Equation (65).

This proposed technique which can render IRFOC tolerant to the short circuit stator fault, is only applicable when the estimated short circuit current is not dangerous for motor winding. The current in the short circuit can be obtained using the estimated variables as follows:

$$\hat{i}_f = \frac{\hat{z}_6}{2/3+\hat{z}_6} \hat{z}_5,$$

where the variables denote:

$$\hat{z}_5 = 2\gamma_a \hat{i}_f /3, \;\; \hat{z}_6 = \hat{f} \;\; \text{and} \;\; \hat{\gamma}_a = \frac{\hat{z}_6}{1+2\hat{z}_6/3}.$$

In order to obtain the best performance and attain a decoupled control between torque and rotor flux, the measured currents $\boldsymbol{i}^{(e)}_{sdq}$ are controlled in the case of healthy conditions when the observer gives the coefficient $\hat{f} = 0$. When the short circuit fault occurs, the estimated coefficient becomes different from zero $(\hat{f} \neq 0)$. This result allows to switch to the control of the $d-q$ axis components of estimated stator current $\hat{\boldsymbol{i}}'^{(e)}_{sdq}$.

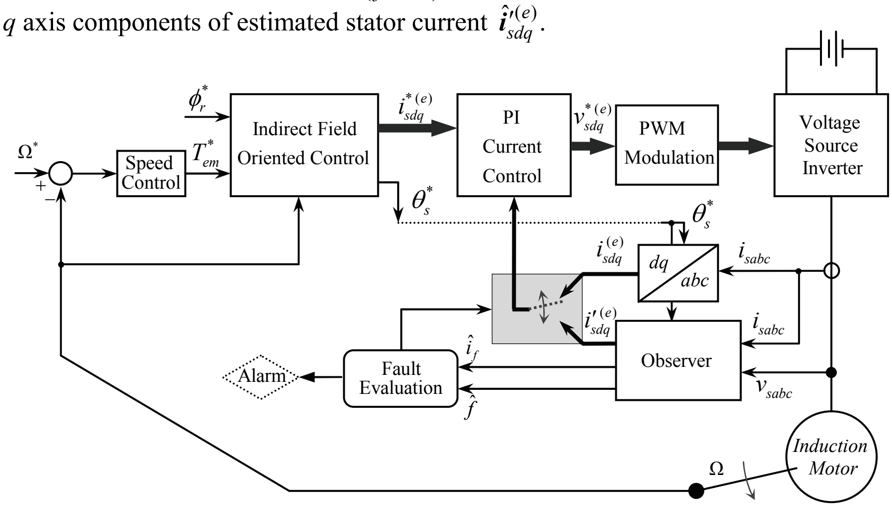

Fig. 3. Speed control and indirect rotor field oriented control scheme with fault tolerant control

Figure 3 shows the structure of field oriented control with speed control and with switch-over strategy, based on the output of the observer, which switches between the control of measured current in case of healthy conditions and estimated currents in the case of faulty conditions.

The feedbacks of measured or estimated $d-q$ axis components of stator current $\boldsymbol{i}_{sdq}^{(e)}$ or $\hat{\boldsymbol{i}}_{sdq}^{\prime(e)}$ are compared with their references, and the errors are sent to current controllers to generate stator voltage references $\boldsymbol{v}_{sdq}^{(e)*}$. The $d-q$ axis components of stator voltage in the synchronous rotating frame are then transformed to the three-phase stator voltages $\boldsymbol{v}_{sabc}^{*}$ for the PWM block.

6. Simulation results and discussions

The technique presented in the previous sections, applied to fault tolerant control of IRFOC for IM has been implemented in the MATLAB/Simulink environment.

The IM used in this study is three phases 0.75 kW with 50 Hz, Y stator windings connection and 400 V power supply. Their electrical and mechanical parameters are shown in Table 1.

Table 1. Parameters of IM adopted for simulation purpose

Description	Parameter	Value	Units
Stator inductance	l_s	0.5578	H
Rotor inductance	l_r	0.6152	H
Mutual inductance	m_{sr}	0.54	H
Stator resistance	r_s	11.8	Ω
Rotor resistance	r_r	11.3	Ω
Rotor inertia	J	2.10^{-3}	$\text{Kg} \cdot \text{m}^2$
Number of pole pairs	p	1	–
Rated load	T_n	2.38	Nm
Rated speed	N_n	2760	rpm
Rated current	I_{sn}	2.5	A
Friction coefficient	F	287.10^{-6}	Nm · sec

The speed controller used is an I-P (Integral-Proportional) controller with output limitation and anti-windup, as shown in Figure 4. The parameters of speed controller were chosen as follows: $k_{p\Omega} = 0.268$, $k_{p\Omega} = 70.79$, in order to obtain fast and precise response in speed tracking.

For d and q current controllers, the following values of parameters of PI (Proportional-Integral) controller are chosen as follows: $k_{pd} = 6.15 \times 10^2$, $k_{id} = 1.5 \times 10^5$, $k_{iq} = 3 \times 10^4$.

The feedback gain of the observer are chosen as:

$$\mathbf{K}_0 = \begin{bmatrix} 0{,}1 & 0 & 1 & 1 & -10 & 0 \\ 0 & 0{,}1 & 1 & 1 & 0 & 0 \end{bmatrix}^T \quad \text{and} \quad \mathbf{K}_1 = \begin{bmatrix} 0 & 0 & 0 & 0 & 0 & 0 \\ 0 & 0 & 0 & 0 & 1{,}1 & 0 \end{bmatrix}^T$$

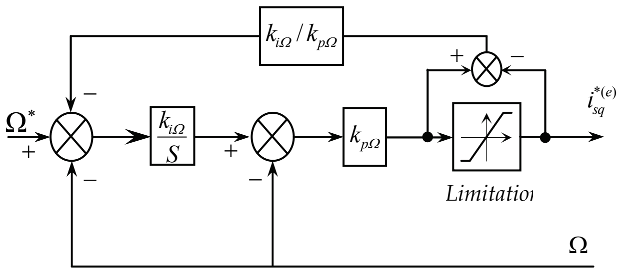

Fig. 4. I-P speed controller scheme with limitation and anti-windup

The simulation test involves the following operating sequences: the rotor flux is required to reach the nominal value $\phi_r^* = 0.653$ Wb and a step change at time $t = 0.3$ sec in the rotor speed of value of 150 rad/s is applied to the IM. To investigate the performances of the IM control, the following disturbances are applied. For test of the performances of IFOC of IM when running without short circuit fault (Fig. 5), only the motor shaft is subject to step torque of 2.38 Nm at time $t = 2$ sec. But for test with fault (Figs. 6, 7), the inter-turn short circuit fault is applied at time $t = 1$ sec with $\gamma_a = 30\%$ fraction of turns short-circuited and the load torque of $T_l = 2.38$ Nm is applied at time $t = 2$ sec.

In Figure 5 following time histories are reported: the speed, the $d - q$ axis components of the stator current in the rotating reference frame with theirs references, the currents measured $\boldsymbol{i}_{sdq}$, the estimated currents $\hat{\boldsymbol{i}}'_{sdq}$ in stationary reference frame, the estimated fraction of turns short-circuited, and the $d - q$ axis components of the rotor flux in the rotating reference frame.

In Figure 5, the speed and the flux trajectories converge to their desired references and the load disturbance is rejected. The plots of the $d - q$ axis components of the stator current shown by Figs. 5c, 5d are the images of the reference rotor flux and the developed electromagnetic torque respectively. These currents show up the oscillations due to the inverter commutations. The $d - q$ axis components in the stationary rotating frame of measured currents $\boldsymbol{i}_{sdq}$ (Fig. 5e) and the estimated currents $\hat{\boldsymbol{i}}'_{sdq}$ (Fig. 5f) are similar in this case where the IM functioned in healthy condition corresponded to estimated fraction of short-circuit $\gamma_a = 0\%$ (Fig. 5g).

Figure 6 shows the responses of IRFOC for IM with inter-turn short-circuit in phase '*a*' and control of measured currents $\boldsymbol{i}_{sdq}^{(e)}$. Note that the speed tracks the reference value adequately in case of healthy condition. But when the short-circuit fault is applied, the speed shows up oscillations around of his reference value (Fig. 6b) which persist after application of load torque. In Figure 6g the value of the estimated fraction of turns in the short-circuit is presented compared with his known value. In this figure, a good fault detection is obtained insensitive to the load torque disturbance. The behavior of the $d - q$ axis components of the estimated rotor flux in the synchronously rotating reference frame is reported in Figure 6h, and it shows that in steady state and in the healthy condition: $\hat{\phi}_{rd}^{(e)} = \phi_r^*$ and $\hat{\phi}_{rq}^{(e)} = 0$. But when the

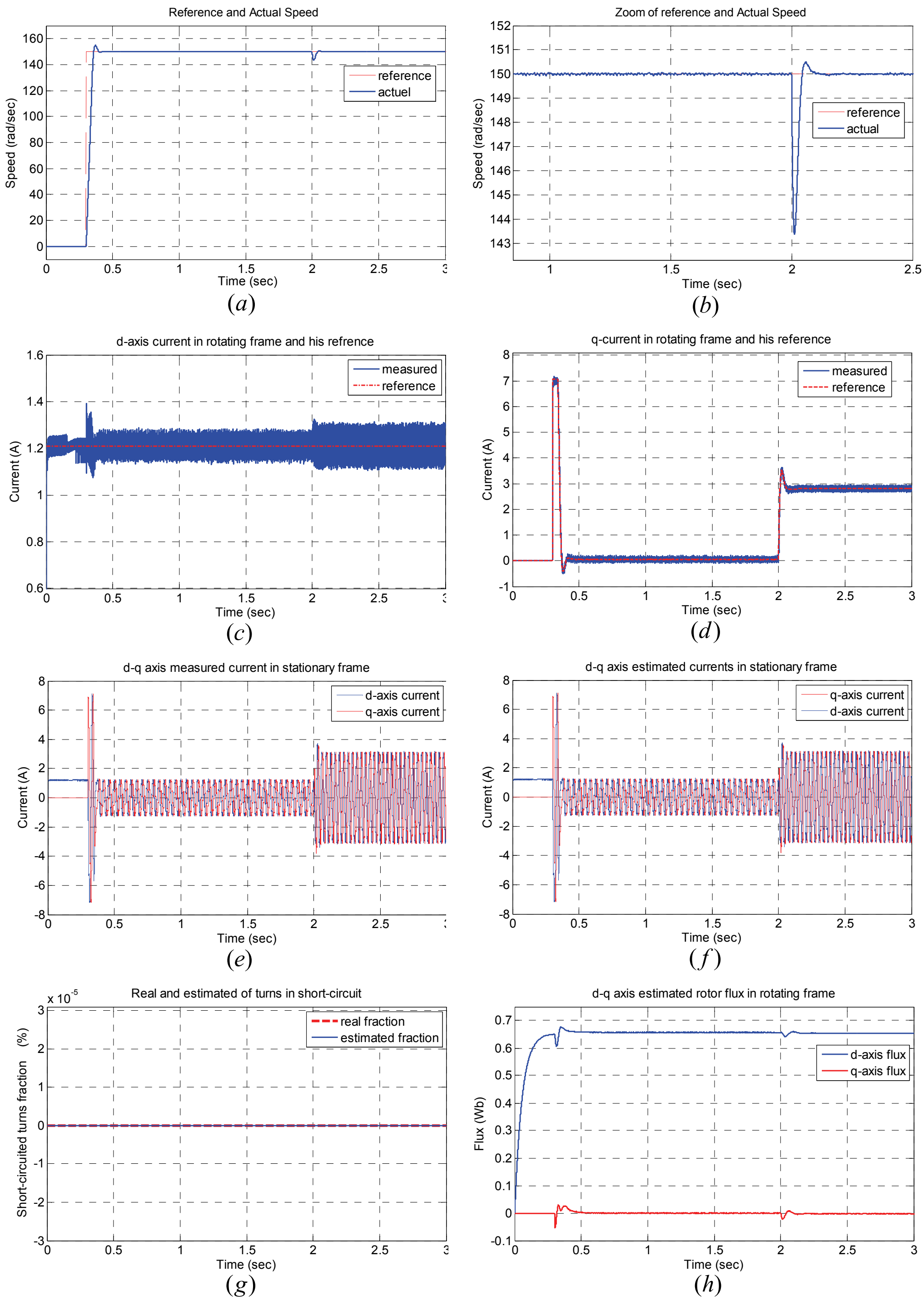

Fig. 5. Simulation results of IRFOC of healthy IM using $\boldsymbol{i}_{sdq}^{(e)}$ measured currents control when a nominal load torque applied at time $t = 2$ sec

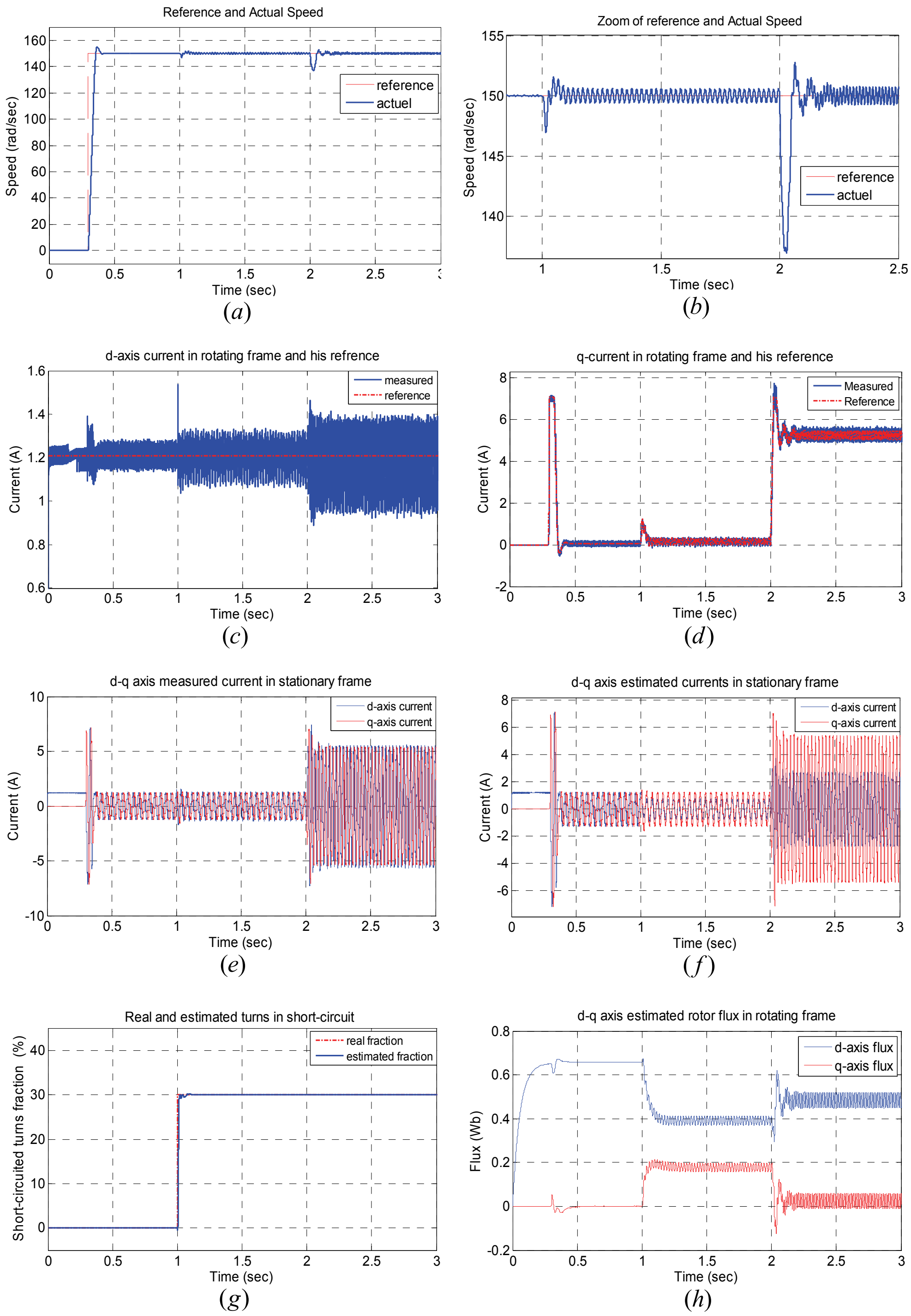

Fig. 6. Simulation results using $\boldsymbol{i}_{sdq}^{(e)}$ measured currents control for IRFOC when a stator fault occurs at time t = 1 sec and a nominal load torque applied at time t = 2 sec

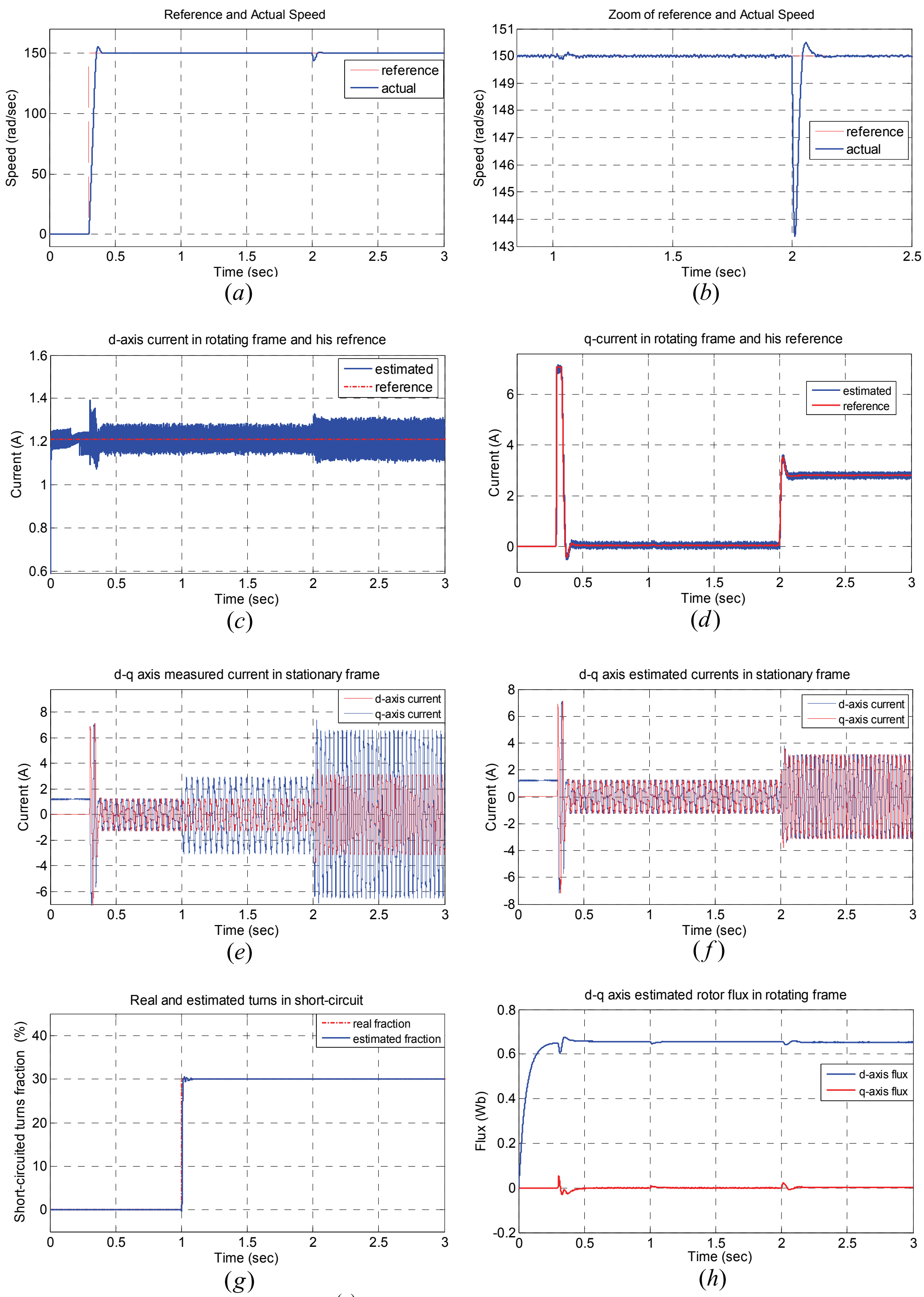

Fig. 7. Simulation results using $\boldsymbol{i}'^{(e)}_{sdq}$ estimated currents control for IRFOC when a stator fault occurs at time t = 1 sec and a nominal load torque applied at time t = 2 sec

short-circuit fault occurs: $\hat{\phi}_{rd}^{(e)} < \phi_r^*$ and $\hat{\phi}_{rq}^{(e)} > 0$, the rotor flux deviates from his reference resulting in a coupling between the torque and flux. We can see an oscillatory behavior from the plots.

The times histories of the IM states presented in the previous figures (Figs. 5, 6) are newly plotted in Figure 7, with making use of the proposed fault tolerant control. When the components of the estimated stator current $\hat{\boldsymbol{i}}_{sdq}^{\prime(e)}$ are controlled instead of measured current $\boldsymbol{i}_{sdq}^{(e)}$, it is clear from the times histories of the speed (Fig. 7b) and rotor flux (Fig. 7h) that the control objectives are normally reached, when the short-circuit occurs in the IM. The speed and rotor flux are tracking the desired reference. The q-axis component of rotor flux remains zero which results in a decoupling between torque and flux and hence in better performance. It is important to note that the oscillatory behavior is easily eliminated by using the proposed FTC from the speed and rotor flux trajectories.

The estimated current flowing through the short circuited, when the IM is controlled with a proposed technique, expressed in per units of the rated stator current is equal to 4,92. For some application, this current can be reduced by associating an appropriate adjustment to the rotating magnetic flux.

7. Conclusion

The problem of oscillations, generated by an inter-turn short circuit fault, in stator winding, in the speed and in the two components of rotor flux and the loss of decoupling between the rotor flux and torque control; for IRFOC; has been solved by a fault tolerant controller using an observer based on the bilinear model of IM with fault. This observer estimates simultaneously the motor states, the amount of turns in inter-turn short circuit and the current flowing in short circuit. In the case of faulty condition we can estimate the new $d-q$ axis components of stator current directly responsible of rotor flux and torque control. The estimated current of short circuit can be evaluated to decide on stopping of the machine or to switch to the control of the new estimated currents.

The above simulation results have demonstrated the effectiveness of the proposed fault-tolerant control.

The proposed technique can be generalized for all three phases, and switches on its own between the control of measured currents and estimated currents in case of faulty conditions.

Though the work proves potential applicability of the fault tolerant control to the induction machine with shorting in stator winding, its practical application is highly limited due to very fast overheating of the shorted sections of the winding.

References

[1] Leonhard W., *Control of electrical drives.* Springer-Verlag, Berlin, Germany (1990).
[2] Vas P., *Vector control of AC machines.* Oxford University Press, London, UK (1990).
[3] Baccarini L.M.R., Tavares J.P.B., de Menezes B.R., Caminhas W.M., *Sliding mode observer for on-line broken rotor bar detection.* Electric Power Systems Research (Elsevier) 80(9): 1089-1095 (2010).

[4] Benbouzid M.E.H., *Review of induction motors signature analysis as a medium for faults detection.* IEEE Trans. on Industrial Electronics 47(5): 984-993 (2000).
[5] Nandi S., Toliyat H.A., LI X., *Condition monitoring and fault diagnosis of electrical motors – a review.* IEEE Trans. on Energy Conversion 20(4): 719-729 (2005).
[6] Benbouzid M.E.H., *Bibliography on induction motors fault detection and diagnosis.* IEEE Trans. on Energy Conversion 14(4): 1065-1074 (1999).
[7] Diallo D., Benbouzid M.E.H., Makouf A., *A fault tolerant control architecture for induction motor drives in automotive applications*. IEEE Trans. on Vehicular Technology 53(6): 1847-1855 (2004).
[8] Williamsons S., Mirzoian K., *Analysis of cage induction motors with stator winding faults.* IEEE Trans. Power Apparatus and Systems 104(7): 1838-1842 (1985).
[9] Kim K., Parlos A.G., *Model-Based Fault Diagnosis of Induction Motors Using Non- Stationary Signal Segmentation.* Mechanical Systems and Signal Processing 16(2-3): 223-253 (2002).
[10] Guldemir H., *Detection of airgap eccentricity using line current spectrum of induction motors.* Electric Power Systems Research (Elsevier) 64(2): 109-117 (2003).
[11] Toliyat H.A., Lipo T., *Transient analysis of cage induction machines under stator, rotor bar and end ring faults*. IEEE Trans. on Energy Conversion 10(2): 241-247 (1995).
[12] Joksimovic G.M., Penman J., *The detection of interturn short circuits in the stator windings of operating motors.* IEEE Trans. on Industrial Electronics 47(5): 1078-1084 (2000).
[13] Fillippetti F., Franceschini G., Tassoni C., VAS P., *Recent developments of induction motor drives fault diagnosis using AI techniques.* IEEE Trans. on Industrial Electronics 47(5): 994-1004 (2000).
[14] Duan G., Patton R.J., *Robust fault detection using Luenberger-type unknown input observers-a parametric approach.* International Joumal of Sysfems Science 32(4): 533-540 (2001).
[15] Koenig D., Mammar S., *Design of a class of reduced order unknown inputs nonlinear observer for fault diagnosis*. Proc. of the American Control Conference, Arlington, USA, pp. 2143-2147 (2001).
[16] Bonivento C., Isidori A., Marconi L., Paoli A., *Implicit fault-tolerant control: application to induction motors.* Automatica 40(3): 355-371 (2004).
[17] Yanf H., Saif M., *State observation failure detection and isolation (FDI) in bilinear systems*. International Journal of Control 67(6): 901-920 (1997).
[18] Edwards C., Tan C.P., *Fault tolerant control using sliding mode observers.* Conference on Decision and Control, Nassau, BAHAMAS, pp. 5254-5259 (2004).
[19] Padmakumar S., Vivek A., Kallol R., *An Investigative Study into Observer based Non-Invasive Fault Detection and Diagnosis in Induction Motors.* World Academy of Science, Engineering and Technology 51 (2009).
[20] Huangfu Y., Liu W., Ma R., *Permanent magnet synchronous motor fault detection and isolation using second order sliding mode observer.* Proc. 3rd IEEE Conference on Industrial Electronics and Applications, ICIEA'2008, pp. 639-644 (2008).
[21] Dongmo J.E., Kwatny H.G., Nwankpa C. et al. *Variable Structure Design of a Fault Tolerant Control System for Induction Motors.* IEEE, Electric Ship Technologies Symposium, ESTS'2007, Arlington, USA, pp. 531-535.
[22] Nasir Uddin M., Wang W., Huang Z.R., *Modeling and Minimization of Speed Ripple of a Faulty Induction Motor with Broken Rotor Bars.* IEEE Trans. on Industrial Appl. 46(6): 2243-2250 (2010).
[23] Fekih A., *Effective fault tolerant control design for nonlinear systems: application to a class of motor control system.* IET Control Theory and Applications 2(9): 762-772 (2008).
[24] Barro R., Hsu P., *Torque ripple compensation of vector controlled induction machines.* Power Electronics Specialists Conference of IEEE, PESC'97, pp. 1281-1287 (1997).
[25] Krause P.C., Wasynczuk O., Sudhoff S.D., *Analysis of Electric Machinery.* IEEE Press (1994).
[26] Tallam R.M., Habetler T.G., Harley R.G., *Transient model for induction machines with stator winding turn faults.* IEEE Trans. on Industrial Applications 38(3): 632-637 (2002).
[27] Kallesøe C.S., Cocquempot V., Izadi-Zamanabadi R., *Model based fault detection in a centrifugal pump application.* IEEE Trans. on Control Systems Technology 14(2): 204-215 (2006).
[28] Lu Q.F., Cao Z.T., Ritchie E., *Model of stator Inter-turn short circuit fault in doubly-fed induction generators for wind turbine.* 35th Annual IEEE Power Electronics Specialists Conference, PESC'2004, Germany (2004).

[29] Kallesøe C.S., Izadi-Zamanabadi R., Vadstrup P., Rasmussen H., *Observer-Based Estimation of Stator-Winding Faults in Delta-Connected Induction Motors: A Linear Matrix Inequality Approach.* IEEE Trans. on Industry Applications 43(4): 1022-1031 (2007).

[30] Benjamin G., *Observateurs et Commande Basée sur un Observateur pour les Systèmes Bilinéaires.* PhD thesis, Henri Poincaré University, Nancy, France (2008).

[31] Cruz S.M.A., Cardoso A.J.M., *The method of multiple reference frames applied to the diagnosis of stator faults in three-phase induction motors*. 4th International Power Electronics and Motion Control Conference, IPEMC' 2004, Xi'an, China (2004).